

Fatigue Life Prediction of Al 7075-T6 Notched Specimens with Circular Holes Using Several Multiaxial Fatigue Criteria

J. Dabbagh Yarishah^{1*} and F. Hosseini Mansoub²

¹Department of Engineering, University of Bonab, Bonab - 5551761167, Iran; jamaldabbagh@bonabu.ac.ir

²Department of Engineering, Maragheh Branch, Islamic Azad University, Maragheh, Iran

Abstract

In this study, Fatigue lives of the specimens with circular holes have been studied on the fatigue life strength of 7075-T6 aluminum alloy specimens via experimental and multiaxial fatigue analysis. The tests of Load controlled fatigue stated samples have been conducted on the servo-hydraulic Zwick/Amsler fatigue testing machine with the frequency of 15 Hz. ANSYS code which defines a finite nonlinear element was chosen as the measure of stress and strain of the specimens which are caused by the loads applied on these specimens. Fatigue lives of the specimens with circular holes were predicted with Kandil-Brown-Miller (KBM), Glinka, Varvani-Farahani (VF), Fatemi-Socie (FS), and smith-Watson- Topper (SWT) multiaxial fatigue criteria by means of the local stress and strain distribution obtained from the finite element analysis. The comparison between experimental results and multiaxial fatigue predictions revealed that among the applied criteria, the Glinka and FS approaches have the best accuracy for the specimens.

Keywords: Critical Plane, Finite Element, Multiaxial Fatigue, Notch

1. Introduction

Stress and strain are the two parameters which affect the mechanistics of the engineering components such as automotive bodies and aircraft components. Regardless of the state of relativity, two or three complex stresses are found at notches of joints which could be defined as geometric “breakpoints”. Multiaxial fatigue should be taken into account as one of the main parameters where it has a critical importance for reliability of the operative system and production of optimized engineering designs.

The term “complex stress” is concerned with principal stresses encountered in notches or joint connections where these are considered as geometric disturbances of a surface. Existence of a multiaxial form of a fatigue is considerable when operation should ly in reliable limits and optimization of engineering components are sine qua non. So, the analysis of multiaxial fatigue gets an important implement for assessing these components of fatigue

strength. Numerous multiaxial fatigue criteria have been suggested in the articles for metals in order to predict fatigue strength of the components. Though, there are several multiaxial fatigue criteria in the articles, researchers frequently meet several trouble in engineering design in using of these criteria. Although it is probable to obtain good fatigue results by the use of multiaxial fatigue criteria, this is not useful for complex multiaxial loadings. These criteria are evaluated for different materials and loadings by Papadopoulos et al.¹, Brown and Miller², You and Lee³, Wang and Yao⁴.

Technically, energy-based and strain-based and stress-based criteria define the basic classification of multiaxial criteria which are used for the estimation of fatigue strength acting on mechanical parts⁵. Stress criteria, theorized by Findley⁶, Susmel and Lazzarin⁷, McDiarmid⁸, Crossland⁹ are useful for consideration of cycle of extreme fatigue when the applied strain is small or deformation is elastic. Brown–Miller model¹⁰, Fatemi-Socie¹¹, Li-Zhang¹² and

*Author for correspondence

Wang– Brown model¹³ that exemplify the strain criteria could be a good consideration wherever the plasticity is of concern. Smith– Watson–Topper model¹⁴, Glinka et al.¹⁵ and Varvani-Farahani¹⁶ suggested the energy-based multiaxial criteria where stress and strain-related considerations are also taken into. With regard to the critical plane concept, multiaxial fatigue criteria could be shaped differently.

From explanations of fatigue cracking behavior have mainly developed the specimens of smooth critical plane models, that display cracks begin and spread in preference of orientations. They noted that an appropriate damage model should relate the observed cracking behaviour with strain components acting on the planes of cracking.

For the definition of multiaxial fatigue criteria, a material plane is used where the stress components show the highest effect. In a consequent phase, the fatigue parameters are defined. The parameters could include the mixture of the stress shaped on the critical plane, shear stress, strain or normal strain. Based on the included consideration, the fatigue parameters are calculated. The multiaxial fatigue criteria are then defined and controlled or tried on the used material plane.

It should be noted that, critical plane models can be energy-based, stress-based, strain- based similar to classical models. The high impair plane on which the fatigue impair factors suppose its maximum rate was distinct look like the critical plane. Plane with the fatigue impair factors takes its maximum rate does not permanently according with the critical plane.

Critical plane is based on the Maximum shearing stress for this parameter. The creation of the strain is evaluated and analyzed for the critical plane. Then, these parameters of strain are used to assume factors of the damage of the critical plane. The need for a physical mechanism for determination of fatigue life criterion was suggested by Socie¹⁷. SWT¹⁴ parameter was adapted for the materials having the tensile-type failures where Socie¹⁷ assumed the growth of the crack is in perpendicular angle to the maximum tensile stress.

Liu¹⁸, Chu et al.¹⁹ suggested which energy criteria should be used in a combination where a critical plane approach is considered.

Glinka et al.¹⁵ and Chu et al.¹⁹ reported that the highest damage parameter and determined the critical plane from the transfiguration of stresses and strains in to planes spaced at same increases. They expressed founded on the SWT factors, shear energy and normal components.

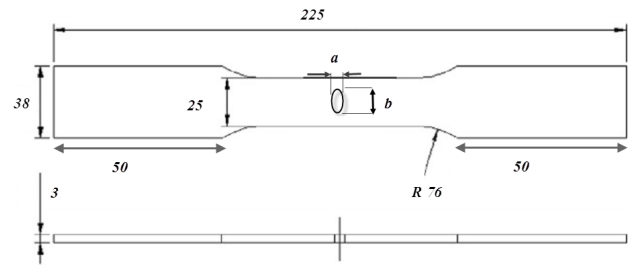


Figure 1. Test specimen configuration for the circular notch $a=b$ (dim. in mm).

Critical plane founded energy factors which are weighted by shear and axial fatigue of the material that suggested by Varvani-Farahani (VF)¹⁶.

In the present study, fatigue life of the Al 7075-T6 notched specimens with circular holes have been predicted using multiaxial fatigue criteria. Application and the dissemination of Stress and strain near the roots of notches could be evaluated by using ANSYS code where the stress and strain are caused by longitudinal loads applied on these locations. Fatigue criteria of multiaxial, KBM, SWT, FS and Glinka and VF were used to predict the fatigue lives of specimens. The prediction was based on the local strain and stress distribution which is analyzed by the use of the finite element.

2. Experimental Procedures

A value of 0.1 for stress ratio and a frequency at 15 Hz were used in fatigue tests with fatigue testing machine of servo-hydraulic Zwick/Roell (Figure 2). Maximum remote longitudinal loads were used as changing parameters of the fatigue tests for each trial. The subsequent average life was displayed in a semi-log S–N diagram in Figure 3.

3. Finite Element Analysis

To assess the fatigue in each specimen, stress and strain should be measured within a close range of the notch root. Multiaxial fatigue criteria are used for assessment of the amount of cycles of the failure. To this end, a 3-D finite element analysis was performed. ANSYS 11²⁰ finite element code was used to acquire the data of distribution for stress and strain in the joint sheets. Figure 4 shows a symmetric 3D finite element model which was meshed

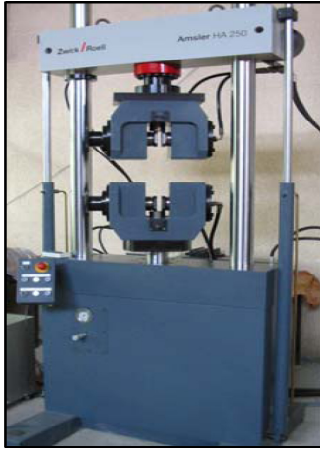


Figure 2. Amsler HA250 kN Fatigue testing machine.

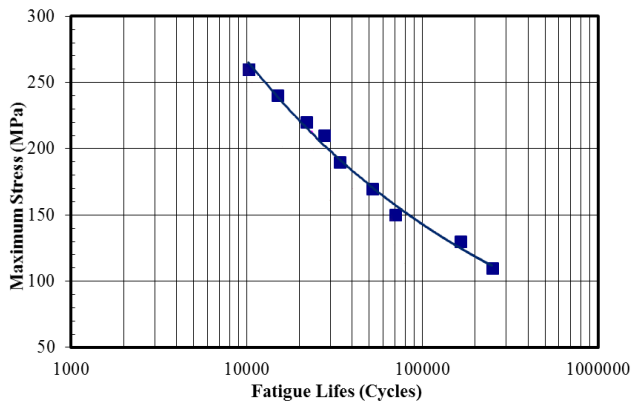


Figure 3. S–N curve attained from experimental fatigue tests for the specimens.

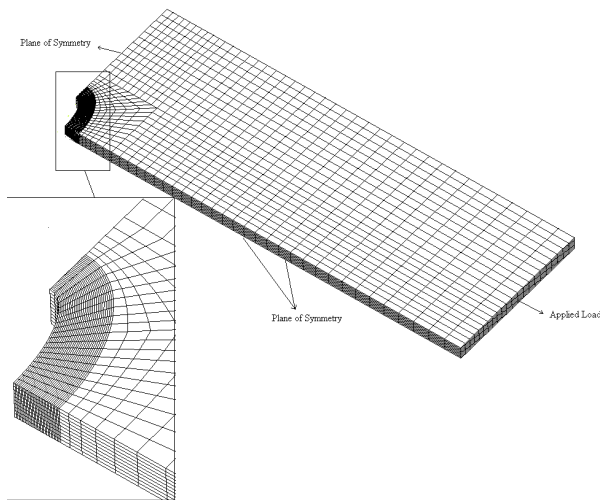


Figure 4. Three-dimensional finite element model and applied boundary conditions.

with Solid95²¹, a twenty-node hexahedral structural solid element. Allied boundary conditions of the model are also given in the figure. In representation of stress and strain behavior of the aluminum alloy 7075-T6, we applied Von Mises criteria for a multi-linear kinematic hardening material. An actual stress-strain curve of the given alloy was used as shown in Figure 5.

To assess the unloading after the mid-cycle state in each cyclic loading, experimentally determined values of minimum force was applied. To measure the deviation from one cycle to the other in stress and strain distribution, the loading/unloading cycle was continued for two cycles. The data of non-linear finite element simulations were used in determination of parameters used in multi-axial fatigue criteria. Data regarding Stresses and strains were obtained from nodes of the area in the vicinity of the notch root. The locus has the highest probability of initiation and amplification. A maximum remote stress of 190 Mpa ($S_{max} = 190 \text{ Mpa}$) was used for the sample of which stress history graphs of its critical node were constructed and demonstrated in Figure 6. The stress near the notch is of a multiaxial form as shown in the figure.

In this research, to estimate the fatigue life of notched specimens, six multiaxial fatigue criteria, i.e. SWT, Glinka, KBM, FS and VF were considered and discussed within the text. In Table-2, material properties for these criteria are given.

4. Smith-Watson-Topper (SWT)

An experimental damage parameter which was assessed at the plane of maximum strain was proposed earlier by Smith et al.

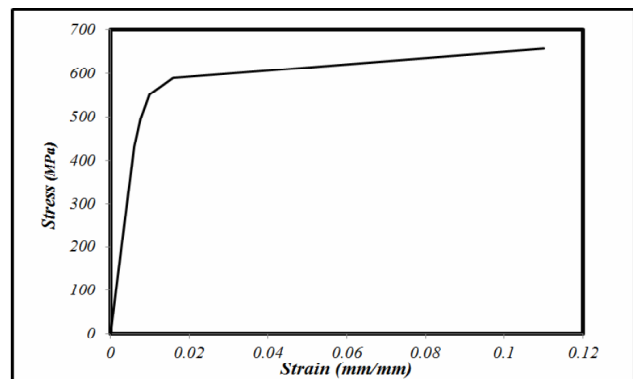


Figure 5. True stress–strain curve of Al 7075-T6.

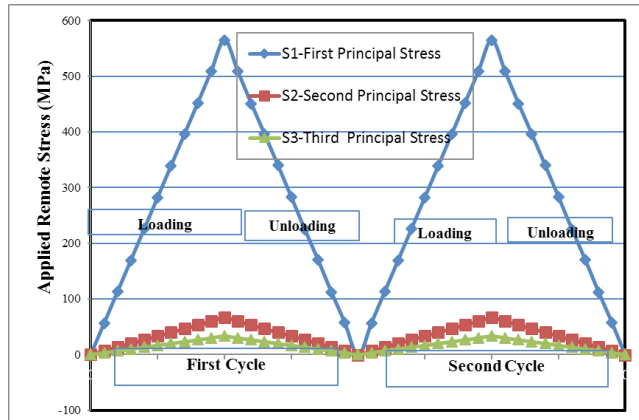


Figure 6. The principal stresses for the typical critical node. stress equals to $\sigma_{max} = 190$ MPa for circular hole specimen.

$$\sigma_n^{max} \frac{\Delta \epsilon_1}{2} = \frac{(\sigma'_f)^2}{E} (2N_f)^{2b} + \sigma'_f \epsilon'_f (2N_f)^{b+c} \quad (1)$$

In the above equation σ_n^{max} and $\Delta \epsilon_1$ are physical basis of SWT parameter could be demonstrated as given in Figure 7a. The maximum value of the product was used in all nodes. At the nodes of FE models, maximum normal stress and principal strain range are calculated in each cyclic loading. Maximum amount of product has been used to calculate the fatigue life using Eq. (1).

5. Kandil, Brown and Miller (KBM)

KBM multiaxial theory: The theory is concerned with the mechanistic explanations of a fatigue crack growth. The parameter of KBM is expressed as;

$$\frac{\Delta \gamma_{max}}{2} + S_k \Delta \epsilon_n = \frac{\sigma'_f}{E} (2N_f)^b + \epsilon'_f (2N_f)^c \quad (2)$$

Plane of the maximum shear strain is considered as the critical plane of the given parameter. Normal strain range of the critical plane is dependent on the shear strain range which defines the “maximum” in KBM theory. Also is a material dependent constant which is chosen so that the equation gives the same fatigue life as for uniaxial stresses. In this work, for Al 7075-T6 gave the best fit.

The values could be obtained from principal stresses and strains of the finite element analysis and Equation (3) and Equation (4) are used for critical nodes located in proximity of the notch root. In these equations, defines the first and thirds principal strains, respectively. Moreover, the equations give information regarding the loading

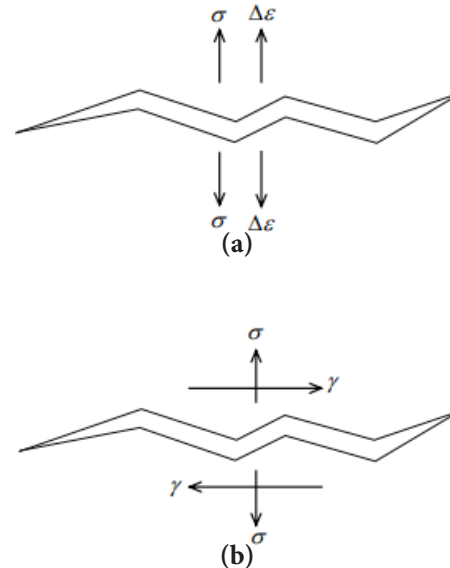


Figure 7. Crack growth: (a) Tensile Crack Growth according to SWT Criterion, (b) Effect of Normal stress on shear Crack Growth according to FS Criterion.

and unloading of a cycle. The parameters are defined in each node and the maximum value in Eq. (2) was used in deducing the fatigue life of each specimen.

$$\frac{\Delta \gamma}{2} = \left(\frac{\epsilon_1 - \epsilon_3}{2} \right) \theta_1 - \left(\frac{\epsilon_1 - \epsilon_3}{2} \right) \theta_2 \quad (3)$$

$$\frac{\Delta \epsilon_n}{2} = \left(\frac{\epsilon_1 + \epsilon_3}{2} \right) \theta_1 - \left(\frac{\epsilon_1 + \epsilon_3}{2} \right) \theta_2 \quad (4)$$

6. Glinka

A sum of elastic and plastic energy densities on the critical shear plane was used to propose a fatigue parameter by Glinka et al.¹⁵

$$\frac{\Delta \gamma}{2} \cdot \frac{\Delta \tau}{2} + \frac{\Delta \epsilon_n}{2} \cdot \frac{\Delta \sigma_n}{2} = \frac{(\sigma'_f)^2}{2E} (2N_f)^{2b} + \frac{E \epsilon'_f}{2} (2N_f)^{b+c} \quad (5)$$

In this proposed method, with finite element analysis, range of shear strain, shear stress range, normal strain range and normal stress range of the critical plane could be determined. Parameters could be determined with Eq. 3, 4, 6 and 7 for nodes near the notch root. In Eq. (5) and the values of the nodes could be used to determine fatigue life.

$$\Delta \tau = \left(\frac{\sigma_1 - \sigma_3}{2} \right) \theta_1 - \left(\frac{\sigma_1 - \sigma_3}{2} \right) \theta_2 \quad (6)$$

$$\Delta\sigma_n = \left(\frac{\sigma_1 + \sigma_3}{2}\right)\theta_1 - \left(\frac{\sigma_1 - \sigma_3}{2}\right)\theta_2 \quad (7)$$

where σ_1 , and σ_3 are the biggest and smallest principal stress values respectively.

7. Fatemi and Socie (FS)

Plane of the maximum shear strain is regarded as the critical plane in this strain-based parameter which is theorized by Fatemi and Socie. Fatemi-Socie fatigue model is as given in (8) maximum shear strain and maximum normal on the plane are used.

occurs. Also is the Fatemi-Socie constant and is the tensile yield strength which can be obtained from uni-axial and torsional tests.

$$\frac{\Delta\gamma_{\max}}{2} \left(1 + k \frac{\sigma_{n, \max}}{\sigma_y}\right) = \frac{\tau'_f}{2G} (2N_f)^b + \gamma'_f (2N_f)^c \quad (8)$$

Torsional fatigue strength, ductility coefficients and shear modules are the coefficients of the theory. The exponent “b” gives torsional fatigue strength and “c” defines ductility exponents of the given parameter calculation. The physical basis of Fatemi-Socie parameter is shown in Figure 7b.

8. Jahed-Varani Method (JV)

In this model²², fatigue damage is measured depending on the summation of plastic and positive elastic strain energy densities. The maximum shear strain range is taken as the critical plane. Normal stress and strain is perpendicular to critical plane. Normal stress and strain is the fatigue damage parameter. Maximum value of fatigue damage parameter occurs on the maximum damage plane, in which normal mean stress measured on the critical plane is defined as in the following Eq

$$\left[\frac{1}{\sigma'_f \varepsilon'_f} (\Delta\sigma_n \cdot \Delta\varepsilon_n) + \frac{1 + \frac{\sigma_n^m}{\sigma_y}}{\tau'_f \gamma'_f} \left(\frac{\Delta\gamma}{2} \cdot \frac{\Delta\tau}{2} \right) \right]_{\max} = \frac{\sigma'_f}{E} (2N_f)^b + \varepsilon'_f (2N_f)^c + \frac{\tau'_f}{G} (2N_f)^b + \gamma'_f (2N_f)^c \quad (9)$$

where the normal mean stress σ_n^m acting on the critical plane is given as follows²²:

$$\sigma_n^m = \frac{1}{2} (\sigma_n^{\max} + \sigma_n^{\min}) \quad (10)$$

Eq. (3) and Eq. (4) are used to calculate normal stress, which is the same with the first principal stress. Eq. (10) was used for calculation of parameters of the critical node. In the left side of the equation, critical node reaches its maximum value.

9. Results and Discussion

As mentioned earlier, in order to obtain the S-N curves of notched specimens with circular notches a series of experimental tests were conducted. For this purpose, fatigue tests were performed with different maximum remote longitudinal loads. Furthermore, in order to predict the fatigue lives based on the selected multi-axial fatigue criteria and finally to compare with those obtained from the experimental fatigue tests, finite element analysis was used to obtain the stress distribution in the specimens due to the longitudinal applied loads.

The predicted fatigue lives and the experimental lives are plotted together in Figure 8 for the specimens. In these figures, the horizontal axis is the experimental life and the vertical axis is the predicted life. Both lives are in log scale. The Predicted results coincide with the values of the experimental set-up. Two other bounds are also indicated with the dashed lines in the given Figure. The inner bound and outer bound are in accordance with the life factor of 2 and life factor 10, respectively.

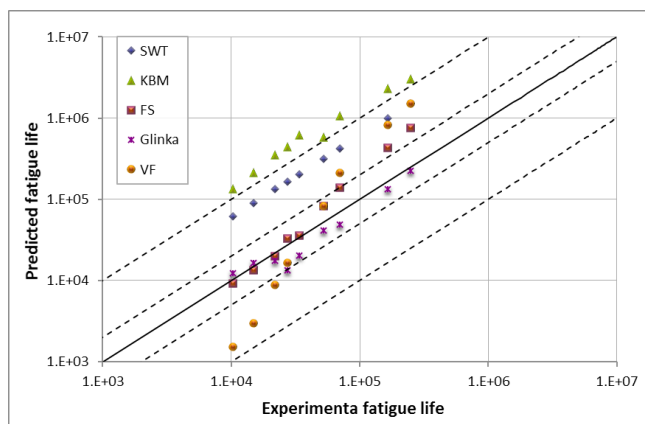


Figure 8. The predicted fatigue lives via multi-axial fatigue criteria versus experimental fatigue lives for the specimens with circular holes.

Table 1. Mechanical properties of 7075-T6 aluminium alloy

Young's modulus (GPa)	Yield stress (MPa)	Tensile strength (MPa)	Poisson's ratio	Elongation (%)
71.5	503	600	0.33	0.11

Table 2. Aluminium 7075-T6 used in multiaxial fatigue criteria

σ_y	ν	E	σ'_f	b	ϵ'_f	c	γ'_f	τ'_f
503 MPa	0.33	71.5 GPa	1466 MPa	-0.143	0.262	-0.619	0.453	846 MPa

Table 3. The average absolute values of errors for selected criteria (in percentage)

multiaxial fatigue criteria	SWT	Glinka	KBM	FS	VF
Specimens with Circular holes	100	16	148	28	127

In Figure 8, results show that our findings have a good correlation with Glinka and FS criteria. Within the figure, majority of the points fall in the range of life factor 2 when Glinka criterion are used while points fall near the range of life factor 2 when FS criterion are used. With the SWT and KBM theories, predictions of fatigue lives are highly deviated. Glinka and FS criteria gave the most accurate prediction for the fatigue life.

Results of the multiaxial fatigue criteria and the experimental test results are compared. An error index is used to give a quantitative and reliable comparison of these results.

$$E = \log \left(\frac{N_{exp}}{N_{pre}} \right) \tag{11}$$

$$\bar{E} = \frac{1}{n} \sum_{i=1}^n |E_i| \tag{12}$$

where N_{exp} is the experimental life and N_{pre} is the predicted life.

The average absolute values of errors in different employed multiaxial fatigue criteria are presented in in Table 3.

Use of Glinka and FS criteria give the most accurate results in all specimens dedicated from the error index. Also, a comparable difference in the level of inaccuracy

for multiaxial fatigue criteria could be seen in application of KBM and VF theories in Table 3.

10. Conclusions

In this paper, in order to investigate the accuracy and performance of the selected multiaxial fatigue criteria, the fatigue life experimental results have been compared with those obtained from the multiaxial analyses. Based on the obtained results, the following conclusions can be drawn from the study:

It was revealed the state of stresses near the notch root is multiaxial.

Experimentally obtained results for the fatigue test were compared with the results obtained by application of multiaxial fatigue criteria. Glinka and FS give the most accurate results whereas KBM and VF lead to inaccuracy for fatigue life prediction with the applied multiaxial fatigue criteria used in this study design.

11. References

- Papadopoulos IV, Davoli P, Grola C, Filippini M, Bernasconi A. A Comparative Study on Multiaxial High-Cycle Fatigue Criteria for Metals. *International Journal of Fatigue*. 1997; 19(3):219–35.
- Brown MW, Miller KJ. Two Decades of Progress in the Assessment of Multiaxial Low-Cycle Fatigue Life. *American Society for Testing and Materials*. 1982; 482–99.
- You BR, Lee SB. A Critical Review on Multiaxial Fatigue Assessments of Metals. *International Journal of Fatigue*. 1996; 18(4):235–44.
- Wang YY, Yao WX. Evaluation and comparison of several multiaxial fatigue criteria. *Int J Fatigue*. 2004; 26:17–25.
- Shamsael N, Fatemi A. Effect of hardness on multiaxial fatigue behaviour and some simple approximations for steels. *Fatigue Fract Eng Mater Struct*. 2009; 32:631–46.
- Findley WN. A theory for the effect of mean stress on fatigue of metals under combined torsion and axial load or bending. *J Eng Ind, Trans ASME*. 1959; 81:301–6.
- Susmel L, Lazzarin P. A bi-parametric Wohler curve for high cycle multiaxial fatigue assessment. *Fatigue Fract Eng Mater Struct*. 2002; 25:63–78.
- McDiarmid DL. A general criterion for high cycle multiaxial fatigue failure. *Fatigue Fract Eng Mater Struct*. 1991; 14:429–53.
- Crossland B. Effect of large hydrostatic pressures on the torsional fatigue strength of an alloy steel. *Proceedings of the International Conference on Fatigue of Metals*. London: Institution of Mechanical Engineers; 1956. p. 138–49.

10. Brown MW, Miller KJ. A theory for fatigue failure under multiaxial stress– strain conditions. *Proc Inst Mech Eng*. 1973; 187(65):745–55.
11. Fatemi A, Socie DF. Critical plane approach to multiaxial fatigue damage including out-of-phase loading. *Fatigue Fract Eng Mater Struct*. 1988; 11(3):149–65.
12. Li J, Zhang ZP, Sun Q, et al. A new multiaxial fatigue damage model for various metallic materials under the combination of tension and torsion loadings. *Int J Fatigue*. 2009; 31:776–81.
13. Wang CH, Brown MW. A path-independent parameter for fatigue under proportional and non-proportional loading. *Fatigue Fract Eng Mater Struct*. 1993; 16:1285–98.
14. Smith RN, Watson P, Topper TH. A stress strain function for the fatigue of metal. *J Mater*. 1970; 5:767–78.
15. Glinka G, Shen G, Plumtree A. A Multiaxial Fatigue Strain Energy Density Parameter Related to the Critical Plane. *Fatigue and Fracture of Engineering Materials and Structure*. 1995; 18:37–46.
16. Varvani-Farahani A. A new energy-critical plane parameter for fatigue life assessment of various metallic materials subjected to in-phase and out-of phase multiaxial fatigue loading conditions. *Int J Fatigue*. 2000; 22:295–305.
17. Socie DF. Multiaxial fatigue damage models. *ASME J Engng Mater Tech*. 1987; 109:293–8.
18. Liu KC. A Method Based on Virtual Strain-Energy Parameters for Multiaxial Fatigue. *Advances in Multiaxial Fatigue*, ASTM STP 1191, In: McDowell DL, Ellis R. editors. American Society for Testing and Materials, Philadelphia, 1993; 67–84.
19. Chu C, Conle FA, Bonnen JF. Multiaxial Stress-Strain Modeling and Fatigue Life Prediction of SAE Axle Shafts. *Advances in Multiaxial Fatigue*. In: McDowell DL, Ellis R, editors. American Society for Testing and Materials, Philadelphia. 1993; 37–54.
20. Swanson Analysis Systems Inc., ANSYS, Release 11, 2007.
21. Swanson Analysis Systems Inc., ANSYS, User's Guide for Revision 11, ANSYS 9 Documentation, ANSYS Element Reference, Part I: Element Library, SOLID95, 2007.
22. Jahed H, Varvani-Farahani A. Upper and lower fatigue life limits model using energy-based fatigue properties. *International Journal of Fatigue*. 2006; 28:467–73.